Joint exploitation potential of offshore wind and wave energy along the south and southeast coasts of China

Yi Wen[1], Bahareh Kamranzad [2,3], Pengzhi Lin[4*]

[1] College of Architecture and Environment, Sichuan University, 24, South Section No.1, Yihuan Road, Chengdu, P. R. China 610065

[2] Hakubi Center for Advanced Research, Kyoto University, Yoshida Honmachi, Sakyo-ku, 606-8501, Kyoto, Japan

[3] Graduate School of Advanced Integrated Studies in Human Survivability (GSAIS), Kyoto University, Yoshida-Nakaadachi 1, Sakyo-ku, Kyoto 606-8306, Japan

[4] State Key Laboratory of Hydraulics and Mountain River Engineering, Sichuan University, 24, South Section No.1, Yihuan Road, Chengdu, P. R. China 610065

* corresponding author's email: cvelinpz@scu.edu.cn

Abstract

There is an increasing interest in co-exploiting marine energies of various types, as it can reduce grid connection and maintenance costs and enhance electricity production. A threefold objective of this work is as follows: i) to investigate offshore wind and wave energy potential, complementarity & synergy, and correlation between the two resources in southern China's coastal region using long-term wind and wave data; ii) to analyze the benefits of wind-wave joint exploitation considering specific offshore wind turbine (OWT) and wave energy converter (WEC); and iii) to propose a new index to determine the suitability for co-developing wind-wave projects. The results show that the Beibu Gulf and Taiwan Strait experience the highest correlation between the two resources, in contrast to the Zhejiang coast that exhibits the lowest one. On the other hand, the east waters of Taiwan and Zhejiang coast have the highest synergy. Moreover, quantitative and qualitative analysis shows that the combined device generates less variable power output and zero

This is a peer-reviewed, accepted author manuscript of the following article: Wen, Y., Kamranzad, B., & Lin, P. (2022). Joint exploitation potential of offshore wind and wave energy along the south and southeast coasts of China. Energy, 249, [123710]. https://doi.org/10.1016/j.energy.2022.123710

production in the areas with low correlation and high synergy than the OWT/WEC operating alone. The suggested best sites for future joint exploitation are along the Zhejiang coast, with the potential of generating nearly 40 GWh/year per combined device of SWT-6.0-154 and 6 MW Wave Dargon.

Keywords: Offshore wind; wave energy; southern China; correlation; complementarity and synergy.

1. Introduction

As a result of increasing energy demand and climate change impacts, there has been significantly growing interest in the development of ocean renewable energies [1,2]. Diversified ocean renewable systems have emerged to enhance the competitiveness of ocean energy [3]. Offshore wind and wave energies are the prospects of ocean renewable energies and can play an important role in mitigating the climate change impacts through renewable electricity generation [2].

Offshore wind farms have expanded at an exponential rate over the last decade, owing to less visual effect as well as greater power potential than onshore ones (e.g., [4–6]). Wave energy has the potential to become a substantial contributor to ocean renewable energy because of the considerably higher ocean energy flux than other marine energy, and wave devices can also be employed for coastal protection and adapt to sea-level rise, compared to traditional coastal protection measures (e.g., [3,7–9]). However, despite the advantages of electricity generation from ocean renewable energies, they also have drawbacks. There are adverse effects on the stable operation of the individual wind/wave power system due to their characteristics of randomness and intermittence in time [1,10]. Moreover, as for wave resources, the extraction technology is still immature and has a high Levelized Cost of Energy (LCOE) [11]. While offshore wind and wave farms are generally developed separately, there are substantial engineering and commercial benefits to deploying them together to i) reduce construction and maintenance costs and improve efficiency by sharing grid connection and infrastructure [12,13], ii) enhance the reliability and stability of the power system by reducing the variation of power output and downtime period [14,15], iii) maximize spatial utilization [2,16], and vi) mitigate structural load and increase accessibility to the offshore wind power system [17,18]. Consequently, the wind-wave joint exploitation has obtained increasing attention and has become an advanced research topic (e.g., [10,12,18–20]).

Resources evaluation is fundamental to develop novel energies and attract investors [19]. Many types of research about joint assessments of offshore wind and wave resources have been conducted in regions including America [21,22], Europe [21,23], Ireland [14,24], Denmark [25], Italy [26] Mediterranean Sea [1], and North Sea [20]. Rusu et al. analyzed spatial distribution of offshore wind and wave energy resources in Latin America and Europe and introduced a Total Harmonic Distortion (THD) index to assess the wind-wave hybrid power smoothing [21]. Kalogeri et al. investigated the wind-wave combined exploitation potential in Europe, and the results indicated that the western offshore areas are the most attractive areas [23]. Ferrari et al. proposed an Exploitability Index (ES-index) to assess the wind-wave joint development potential considering both combined energy potential and their correlation [1]. Azzellino et al. assessed co-locate wind and wave resources in the Italian seas and the results showed that the areas with lower correlation are more interesting for the combined energy harvesting [26]. Although this review concludes many benefits and potential areas of wind-wave joint development, the investigation of that and the relationship between wind and wave in time and space are still insufficient in many regions including China sea. In addition, the technological combination of wind energy with wave energy is far from mature to commercial applications. There are few offshore wind-wave hybrid systems in operation across the world. For example, Denmark’s Floating Power Plant AS has developed the Poseidon Floating Power, which is the first successful offshore-tested combined wind-wave device in the world [27], and the W2 Power, manufactured by Norway's Pelagic Power AS, offers the first feasible solution for combining offshore wind and wave energy conversion technology [28].

As China is a large marine country that has 18,000 kilometers of mainland coastline, it has enormous potential in terms of its wave and offshore wind energy resources [29]. Several types of analysis on estimations of wave (e.g., [3,30–37]) and offshore wind resources (e.g., [37–43]) around China have been carried out. Chen et al. investigated offshore wind and wave resources in the nearshore areas of Shenzhen based on buoy observational data and the results revealed that wave energy development potential in the investigated sites is limited [34]. Wang et al. analyzed annual, seasonal and monthly wind and wave resources characteristics in the South China Sea [35]. Zheng et al. [37] and Dong et al. [43] examined the wind and wave resources in the China sea, finding that wind energy is greater in the southeast of the Yangtze River Delta than that in the northwest [37,43]. Wan et al. assessed the joint development potential considering hybrid installed capacity in the South China Sea for the first time, while the relationship between wind and wave energy had not been considered [44]. In addition, many offshore wind power projects have now been implemented along China's coast [45], and a wave energy full-scale field has been tested in Guangdong [46]. However, little work has been done in China when it comes to combined wind and wave resource exploration. Wind-wave joint exploitation in China is a recent topic, and thus very limited studies have been conducted [44]. Hence, it is essential to jointly analyze offshore wind and wave resources in China to fill this fundamental literature gap, investigate how they might interact, identify attractive areas for combined energy exploitation in the future, and estimate the joint exploitation potential.

This study will depend on wind reanalysis and simulated wave data from the Japanese 55-year Reanalysis (JRA-55) [47] and the authors' previous work [48], respectively. The time scale from 1958 to 2012 will be used for wind and wave resources analysis. The energy potential of offshore wind and wave resources will be analyzed on annual and seasonal scales, and the correlation and complementarity & synergy between two resources in the southern China's coastal region will be investigated for the first time. In addition, given an OWT (SWT-6.0-154) and a WEC (6 MW Wave Dragon), the improvement of co-exploitation of wind and wave resources over wind or wave independent development will be evaluated by comparing energy production, capacity factor, zero production and variability of power output. Finally, a new approach combining wind and wave power potential, correlation and synergy between the two resources will be suggested. This study aims to identify potential and suitable areas for future investments in wind-wave combined systems and hence for offshore farm installations.

2. Materials and methods

2.1 Study area and data source

This investigation is focused on the southern China (Fig. 1), which covers from the Beibu Gulf in the east to the south of Hangzhou Bay in the west, and the coastal areas with depths below 60 m as a recommended depth for many offshore devices [49–51]. This domain has a long coastline that opens up great opportunities for offshore energies [29], and abundant offshore wind and wave resources have been demonstrated [40,48] and hence it makes the domain an excellent potential for developing offshore renewable energy projects.

In this study, both the wind and wave data cover a 55-year period. The wind data applied for the offshore wind resource analysis is obtained from JRA-55, which is the second atmospheric reanalysis of the global climate produced by the Japan Meteorological Agency (JMA) [47]. This dataset has been previously validated based on a great amount of measured data [47] and used by other researchers (e.g., [3,40,48,52–54]). It has 0.56° and 6 hr spatial and temporal resolutions, separately [55]. The simulated wave data is generated from the Simulating WAves Nearshore (SWAN) model and has 0.05° and 6 hr spatial and temporal resolutions, separately [56]. Moreover, available observations have been employed to validate the wave model. More information on the model setup and verification has been previously given in Ref. [48].

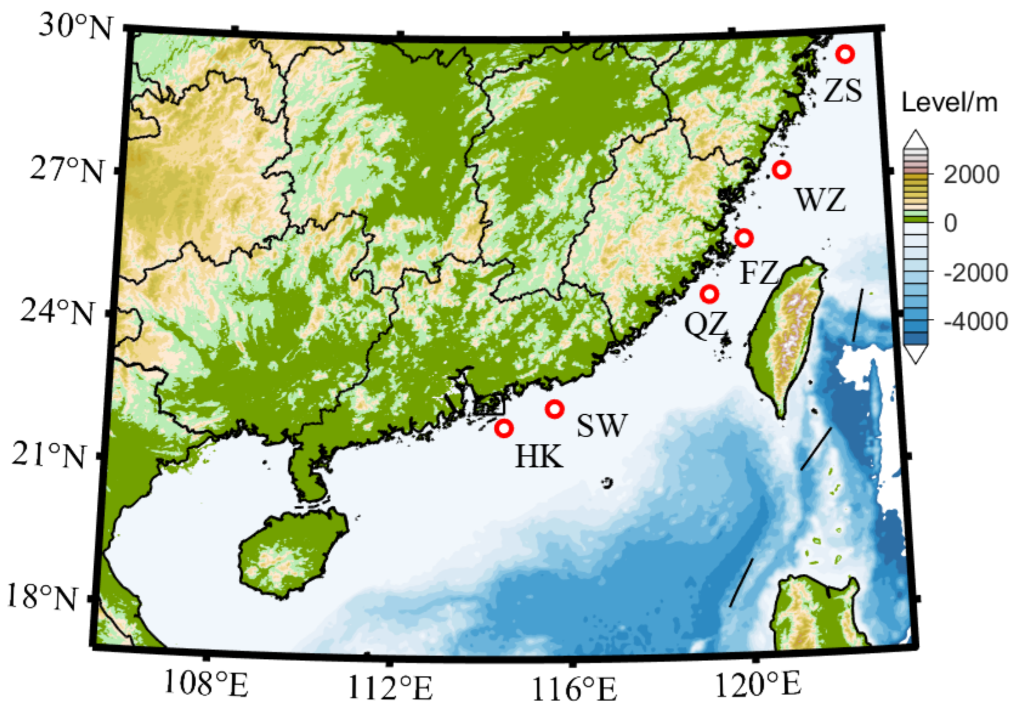

Fig. 1. The bathymetry and the locations of the selected sites of the study area.

2.2 Selection of OWT and WEC

For the exploitation of wave energy resource, a 6 MW Wave Dargon is selected, which is a large-scale, floating, slack-moored energy converter of the overtopping type [57]. It has also been recommended for wave energy extraction in offshore areas due to the suitable performance in the previous work [48]. Table 1 shows the power matrix and performance characteristics of the Wave Dargon. The same capacity, i.e., 6 MW, is adopted for OWT as required to conduct a fair appraisal of the energy output from the two resources. Hence, the SWT-6.0-154 developed by Siemens Wind Power A/S, a manufacturer from Denmark (designs for onshore and offshore wind conditions), is selected. This kind of devices has also been widely installed in the China Sea [58]. The details of the power curve and main characteristics of the SWT-6.0-154 are shown in Table 2. Given the power curve of OWT and the wind speed at hub height, the ultimate power output can be estimated [59].

Table 1. Power matrix of the 6 MW Wave Dargon and the main characteristics.
(Source: www.wavedragon.co.uk)

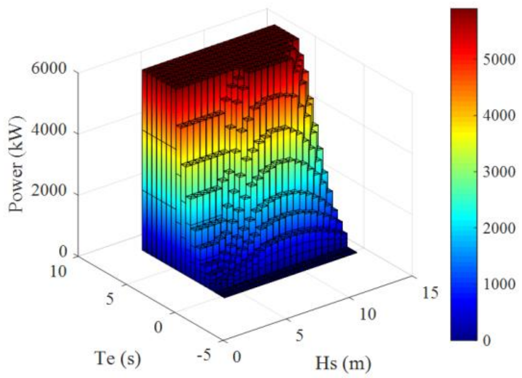

Rated power	6000 kW
Classification	Terminator
Matrix resolution ($H_s \times T_e$)	0.5 m × 0.5 s
Installation depth	> 20 m

Table 2. Power curve of the SWT-6.0-154 and the main characteristics.
(Source: https://en.wind-turbine-models.com/turbines/657-siemens-swt-6.0-154)

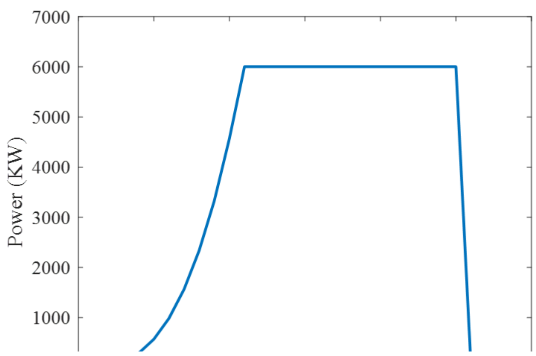

Rated power	6000 kW
Cut-in wind speed	4 m/s
Cut-out wind speed	25 m/s
Rotor diameter	154 m

Swept area	18,600 m²

2.3 Analysis methodologies

Wind energy potential is estimated through wind power density (WPD), and it is calculated as follows [60]:

$$\mathrm{WPD} = \frac{1}{2}\rho_a U^3 \tag{1}$$

where ρ_a is the air density (1.225 kg/m^3 in this study) and U is the wind speed at hub height. Since the JRA-55 model only includes wind field at 10 m, the wind speed extrapolation formula is used in this study [47]. However, previous studies have shown that the height of available wind resources for OWTs is usually between 70 and 100 m (e.g., [6,60]). Therefore, 100 m and power law are chosen as the reference height and wind speed extrapolation, respectively [39,40,61]. The power law applied reads [62]:

$$U = U_r \left(\frac{Z}{Z_r}\right)^{\alpha} \tag{2}$$

where U and U_r are the wind speed at raw height Z and reference height Z_r, respectively. α is the wind shear exponent, and α=0.11 is applied in this study ([63]).

The wave power flux (WPF) is employed to estimate wave energy potential. It can be determined by [3,48]:

$$\mathrm{WPF} = 0.49 H_s{}^2 T_e \tag{3}$$

where H_s and T_e are the significant wave height and energy period.

The correlation is used to assess the potential of resource diversity to reduce power variability [21–23]. The sites where the correlation between the two resources is medium to low are more attractive, as indicates that the peaks in the two resources do not coincide [23]. The correlation coefficient is calculated as follows [23]:

$$R = \frac{1}{N}\sum_{i=1}^{N} \frac{\left(P_{wind,i} - \overline{P}_{wind}\right)\left(P_{wave,i} - \overline{P}_{wave}\right)}{\sigma_{P_{wind}} \sigma_{P_{wave}}} \tag{4}$$

where $\overline{P}_{wind}$ and $\overline{P}_{wave}$ are the mean values of WPD and WPF, respectively, and $\sigma_{P_{wind}}$ and $\sigma_{P_{wave}}$ are the standard deviation of WPD and WPF, respectively.

The correlation coefficient has been previously used to assess the complementarity between different resources, such as wind and solar [64–68], hydro and wind [60], offshore wind and wave [24]. In this study, a method based on the occurrence rate of offshore wind and wave resources above their respective electrical generation threshold (EGT) is applied to evaluate the complementarity and synergy between the two resources in southern China. A similar method has been employed in previous studies for wind and solar resources (e.g., [69,70]). In this study, the power curve/matrix of many widely used OWTs/WECs are investigated, and the EGT for wind/wave resource is defined according to max starting wind speed/pairs of H_s and T_e of OWTs/WECs. When the value of WPD/WPF is less than the EGT, the availability and persistence of the resource could not meet the development of the resource [69]. For offshore wind resource, when wind speed is higher than 5 m/s, i.e., the WPD is higher than 80 W/m^2, it is considered as available for most modern offshore wind turbines [6,40,71]. Therefore, 80 W/m^2 is applied for wind EGT in this study. Similarly, for wave resources, it is worth exploitation when the WPF is greater than 2.5 kW/m (corresponding to H_s >1 m and T_e >5 s) after investigating many WECs and hence the EGT for wave resources is set 2.5 kW/m [50,71–73].

The different indices are defined as follows:

(i) Wind complements wave (WICWA):

$$WICWA = \frac{Number\ of\ hours\ (P_{wind} > 80W/m^2\ \ and\ P_{wave} < 2.5kW/m)}{Total\ number\ of\ hours} \tag{5}$$

This index indicates the occurrence of wind resources complementing wave resources. A high value of WICWA denotes strong wind to wave complementarity and hence only wind farms are suggested in the specific area.

(ii) Wave complements wind (WACWI):

$$WACWI = \frac{Number\ of\ hours\ (P_{wind} < 80W/m^2\ \ and\ P_{wave} > 2.5kW/m)}{Total\ number\ of\ hours} \tag{6}$$

This index indicates the occurrence of wave resources complementing wind resources. A high value of WACWI denotes strong wind to wave complementarity and hence only wave farms are suggested in the specific area.

(iii) Wind and wave synergy (WIWAS):

$$WIWAS = \frac{Number\ of\ hours\ (P_{wind} > 80W/m^2 \text{ or } P_{wave} > 2.5kW/m)}{Total\ number\ of\ hours} \tag{7}$$

This index indicates the occurrence of wind and wave resource synergy. A specific area with high values of WIWAS indicates less intermittency of power output and hence the wind-wave project is highly recommended here.

The power output (P_t) and capacity factor (CF) for each OWT and WEC are examined to determine the electricity generation and energy conversion efficiency of these resources. The actual energy production is equal to power output times the number of available hours for the OWT or WEC, and the power output of OWT (WEC) can be estimated according to the power curve (matrix) and the wind speed (H_s and T_e pairs). Moreover, the CF employed in this study reads [6]:

$$CF = \frac{\overline{P_t}}{P_e} \tag{8}$$

where P_e is the rated power of the OWT or WEC, and $\overline{P_t}$ is the mean values of power output.

The coefficient of variation (CoV) primarily indicates energy stability, which is important to evaluate resources since it is linked to energy output, conversion efficiency, and the longevity of offshore devices [40,50]. It can be calculated as follows:

$$CoV = \frac{\sigma_{P_t}}{\overline{P_t}} \tag{9}$$

where σ_{P_t} is the standard deviation of power output from offshore OWT or WEC.

Several indices have been suggested to detect the favorable locations for combined energy exploitation in previous studies (e.g., [1,21,74]). In this study, a new index, i.e., wind and wave joint exploitation (WWJE), is developed based on the previous method [1] but taking synergy into account. The WWJE can be calculated as the following equation:

$$WWJE = \frac{(C_{wind}\frac{\overline{P}_{wind}}{\overline{P}_{wind}\big|_{\max}} + C_{wave}\frac{\overline{P}_{wave}}{\overline{P}_{wave}\big|_{\max}})WIWAS}{e^{R}} \tag{10}$$

in which, C_{wind} and C_{wave} are weighted factors of WPD and WPF, respectively, and the sum of C_{wind} and C_{wave} is 1. The determination of C_{wind} and C_{wave} depends on the weightage of wind and wave power usage and it will be further discussed in Section 3.5 through sensitivity analysis. $\overline{P}_{wind}$ and $\overline{P}_{wave}$ are (55-year) mean values of wind and wave power, respectively. The dimensionless forms of average wind and wave power are applied by dividing them by their corresponding maximum value in the domain and given different weights due to different conversion efficiency of the resources [1]. Theoretically, the values of R ranges between -1 and 1. Hence an exponential function is used to ensure the output values are always positive with the same monotonicity. Overall, the value of WWJE ranges between 0 and e, and a large value of WWJE indicates a strong recommendation for developing wind-wave combined projects.

3. Results and discussion

3.1 Wind and wave power potential

This section provides a univariate investigation of the domain's offshore wind and wave energy potential. As illustrated in Fig. 2, wave and offshore wind energy have a great potential in southern China, especially in the eastern areas. In Fig. 2a, the largest values of mean WPD are depicted in the Taiwan Strait (above 1200 W/m^2), whereas the southeast waters of Taiwan Island have a very high wave resource (around 25 kW/m) (Fig. 2b). According to this figure, the offshore wind energy potential exhibited in the present study is not much different from that published by Nie and Li. [75] and Wan et al. [44]. The map of wave power potential in the domain showed in this study is also in line with the ones found by Mirzaei et al. [30] and Lin et al. [36].

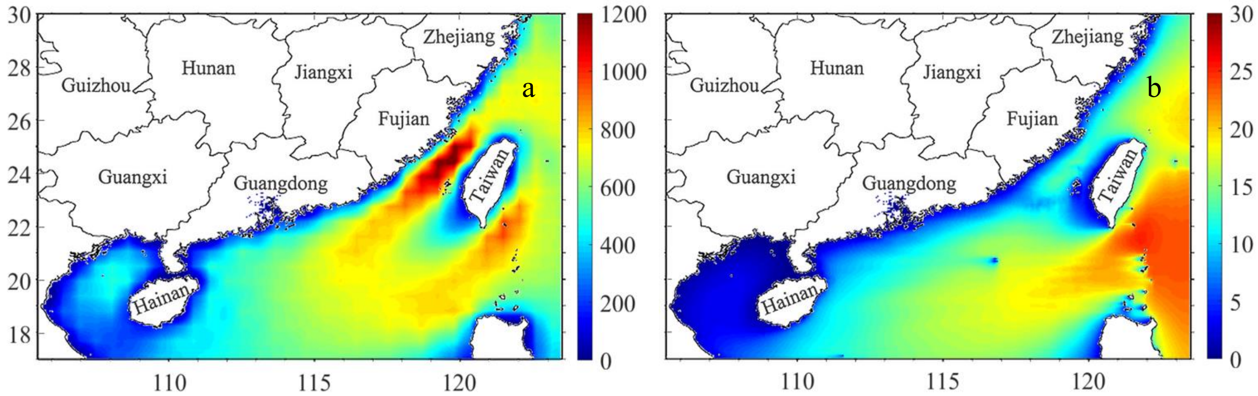

Fig. 2. The spatial distribution of 55-year mean values of (a) WPD at 100m (W/m^2) and (b) WPF (kW/m).

In order to obtain preliminary estimates of the wind and wave potential stability throughout a year, the seasonal mean values of wind and wave potential are obtained (Figs. 3 and 4, respectively). As shown in Figs. 3 and 4, offshore wind and wave potential show significant seasonal variability. Winter has the highest potential for offshore wind and wave resources extraction, with WPD and WPF reaching above 2000 W/m^2 and 38 kW/m, respectively. In contrast, the lowest potential for both resources is encountered during summer. The results are consistent with that of Wang et al. [35] and Wan et al. [76]. Moreover, due to the geographical barrier Taiwan island, the Taiwan Strait is the most promising part of wind energy exploitation throughout one year, whereas it is not the case for wave energy. The least energetic waves occur in the Beibu Gulf in all seasons (less than 5 kW/m), and developing the wave energy is not suggested there.

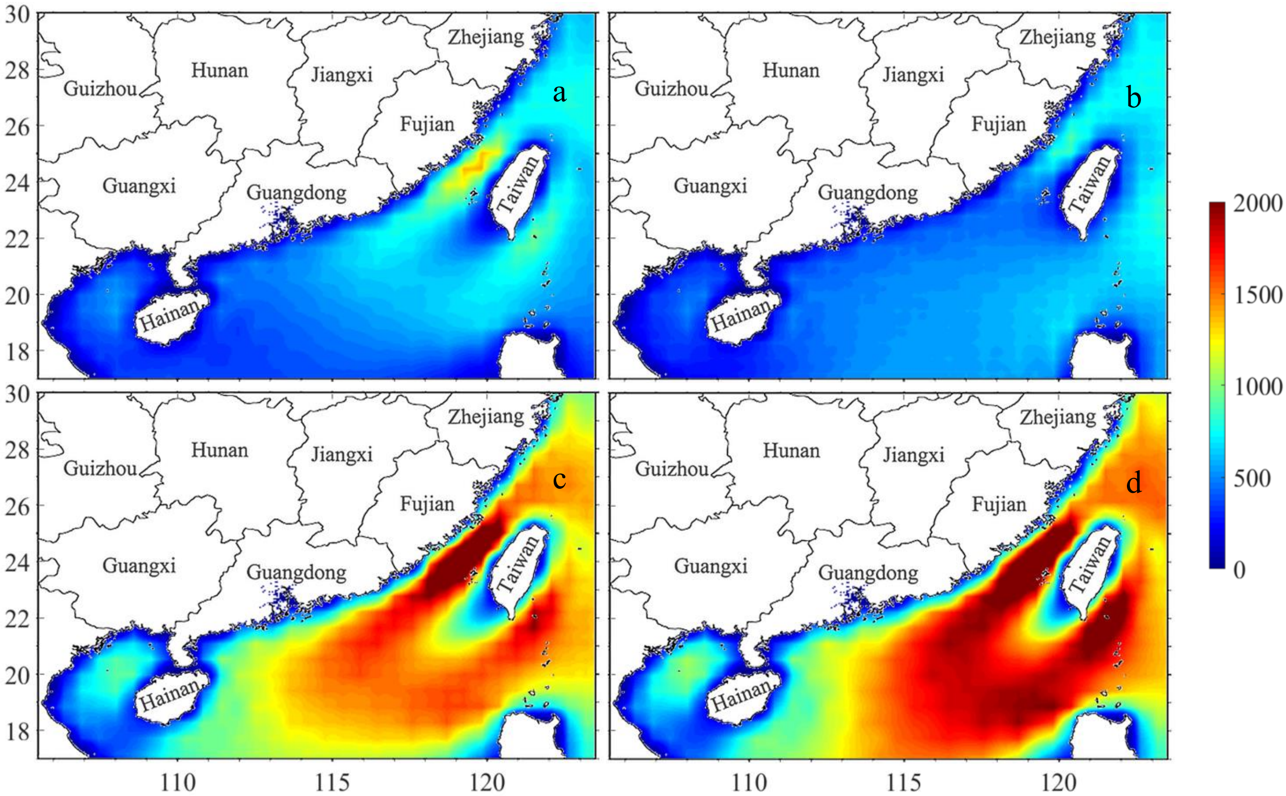

Fig. 3. Seasonal mean values of WPD (W/m^2) in (a) spring (MAM), (b) summer (JJA), (c) autumn (SON), (d) winter (DJF).

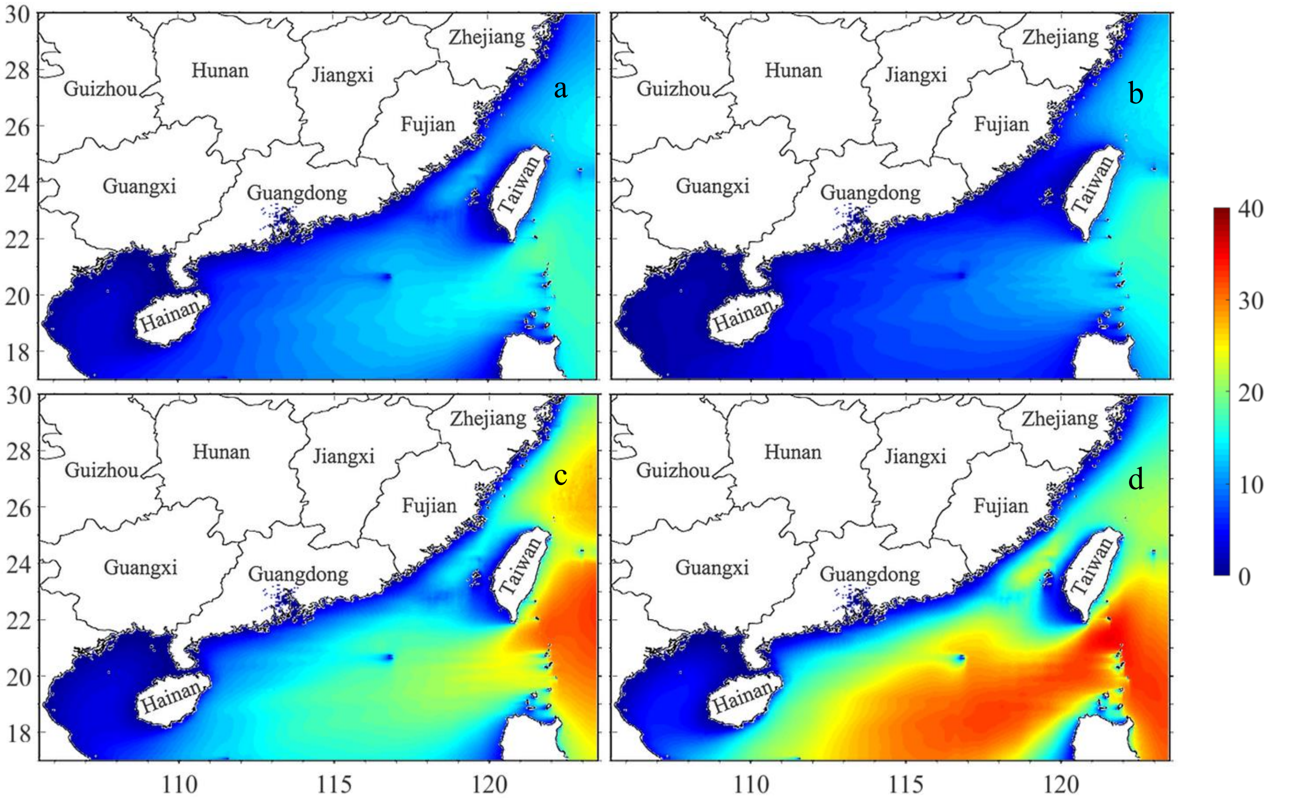

Fig. 4. Seasonal mean values of WPF (kW/m) in (a) spring (MAM), (b) summer (JJA), (c) autumn

(SON), (d) winter (DJF).

3.2 Correlation between wind and wave resources

The joint exploitation of different offshore resources can increase energy yield [1,77] and reduce the power output variability, especially when the resources have a low or negative correlation [22,23,69], thereby contributing to better use of diverse resources and more stable electrical output. Hence, the correlation coefficient R in Eq. (4) on annual and seasonal scales is calculated and shown in Figs. 5 and 6.

As shown in Fig. 5a, a high correlation can be found in most offshore regions, as expected for wind-generated waves. However, there is a relatively moderate correlation (0.6-0.7) between wind and wave resources in the nearshore areas of Zhejiang and on the southeast coast of Taiwan. The reason is the dominance of swells traveling from the Northwest Pacific Ocean [3]. On the other hand, in the sheltered areas, such as the Beibu Gulf and Taiwan Strait, the wave resource is chiefly generated by local wind growth, and hence, it is strongly linked to the wind environment.

The correlation on the south and southeast coasts of China is highlighted in Fig. 5b, the lowest correlation along China's coastlines meets on the Zhejiang coast, closely followed by the Guangdong coast, which makes these regions suitable candidates for wind-wave joint exploitation.

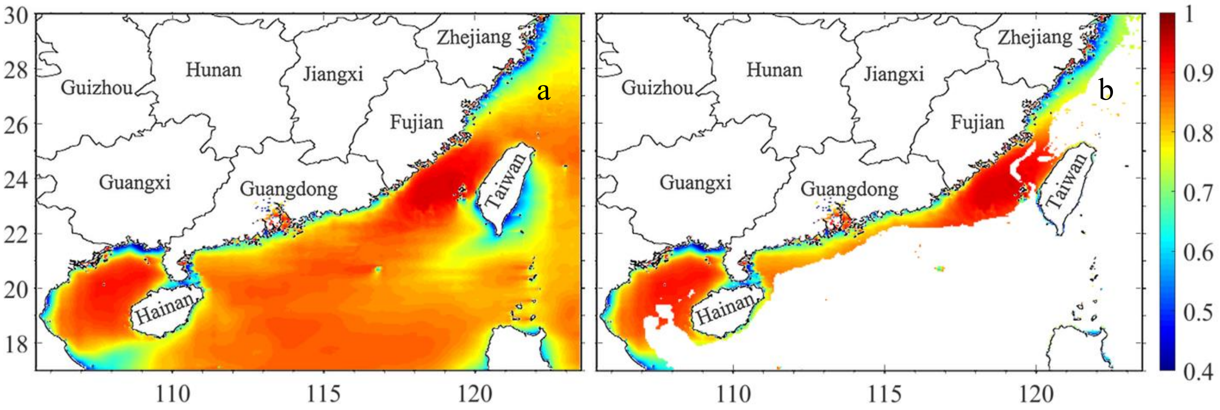

Fig. 5. The spatial distribution of the correlation between wind and wave power in the whole period in (a) the entire domain and (b) the nearshore areas with depths below 60 m.

The seasonal correlation in the domain is reported in Fig. 6. According to this figure, the correlation varies with season, with summer and winter showing the highest and lowest levels, respectively. A relatively low correlation (0.4-0.6) can be found in spring and winter in most areas. It is because that the wave climate in the those areas is usually impacted by the swells originating from the Northeast Pacific Ocean [48]. In autumn, the correlation is relatively high in the southern coasts of China but moderate in the central part of the domain and southeast waters of the Taiwan Island because the wave climate is mainly affected by swells propagating from the southern South China Sea and Northeast Pacific Ocean [48]. In most areas, it is worth noting that the high value of correlation reported during summer corresponds to the low values of both wind (Fig. 3b) and wave power potential (Fig. 4b).

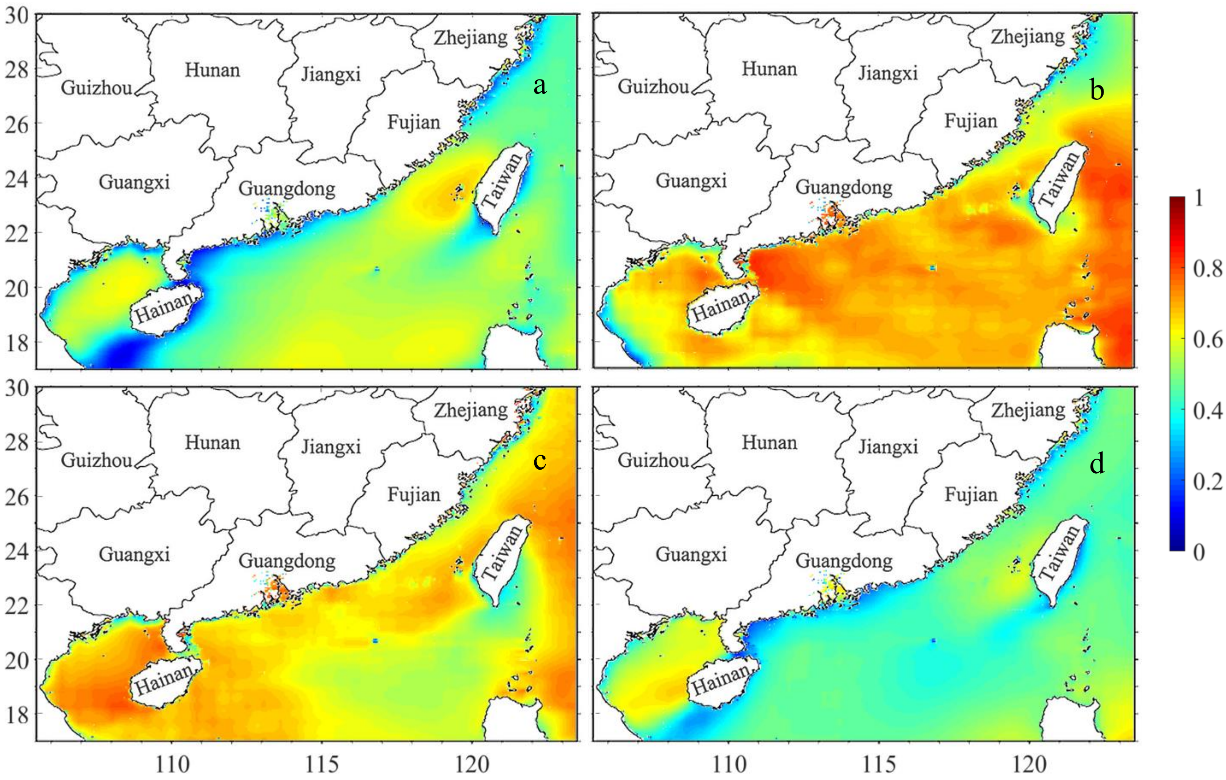

Fig. 6. The spatial distribution of seasonal correlation between wind and wave power in (a) spring (MAM), (b) summer (JJA), (c) autumn (SON), (d) winter (DJF).

3.3 Complementarity and synergy

Three different indices for the complementarity and synergy between the two resources in the domain are depicted in Fig. 7. According to Fig. 7a, the Beibu Gulf is the area where wind complements wave resources in a high degree (around 0.5), which indicates that a wind farm could supply around 4380 h of power per year lost due to loss of wave generation in this area. Besides, some coastal areas such as Zhujiangkou, Fujian coast, and Zhejiang coast meet high WICWA, and hence wave farms are not suggested in those areas. However, the central and east parts mostly show weak and moderate WICWA (< 0.2). Interestingly, an opposite regional distribution with the WACWI can be seen from Fig. 7b. Most of the central and eastern parts, except the Taiwan Strait and Guangdong coast, show relatively high WACWI (around 0.3), indicating a wave farm could generate around 2826 h of power per year lost due to loss of wind generation in this area. However, low WACWI (nearly 0) occurs in the Beibu Gulf and Taiwan Strait.

As shown in Fig. 7c, the temporal synergy between wind and wave resources becomes stronger from west parts to east parts and meets the highest value (nearly 1) in the areas close to the western border of the domain. Clearly, the southeast coast of Fujian, Zhejiang coast, and east coast of the Taiwan are significantly synergetic, and thus, they are attractive areas for wind-wave projects. However, from the perspective of technology, the areas characterized by low values of WIWAS, such as the nearshore areas of the Beibu Gulf and Qiongzhou Strait, are not recommended for further consideration as regards wind-wave projects, since neither wind nor wave source satisfies the effective energy production.

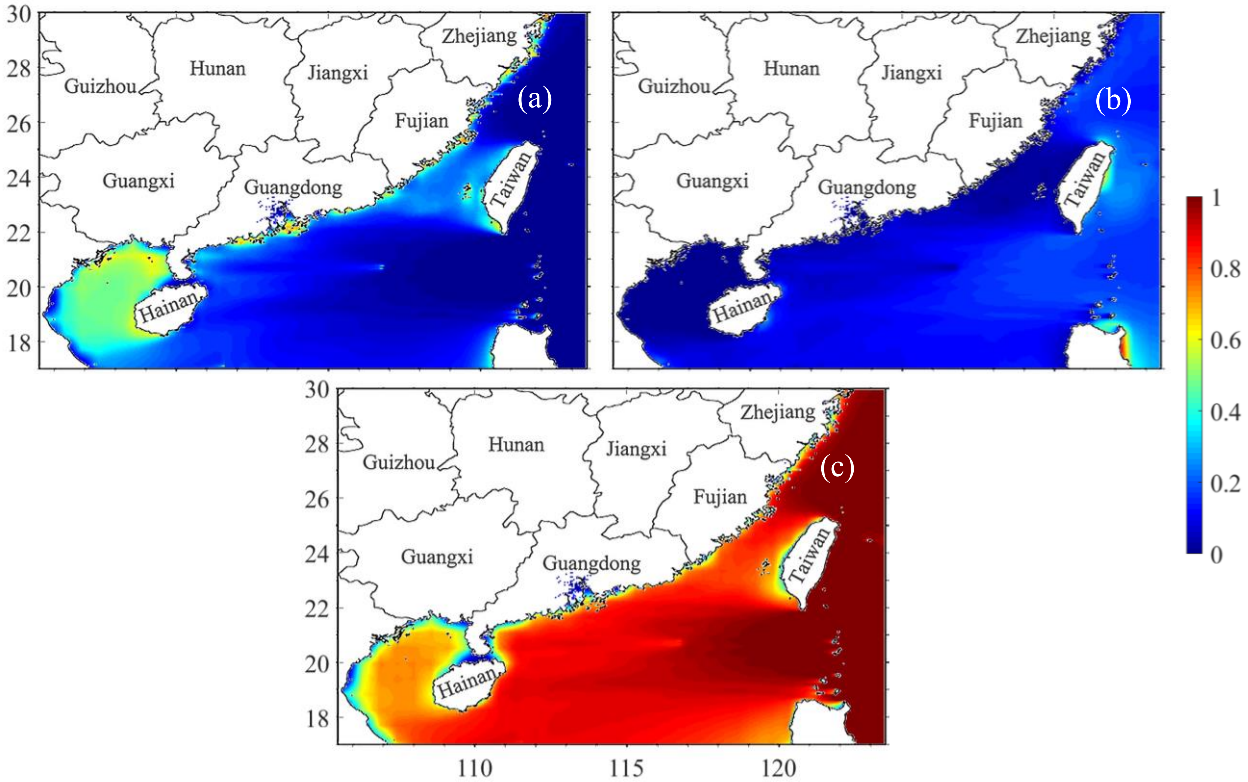

Fig. 7. Complementarity and synergy aspects for (a) WICWA, (b) WACWI, (c) WIWAS.

3.4 Practical wind-wave joint exploitation considering actual OWT/WEC devices

The previous section has investigated the theoretical power resource. On this basis, the possible improvements of wind-wave joint exploitation are assessed considering the single OWT/WEC and their hypothetical combination in terms of energy production, capacity factor, intermittency, and variability. The regions with depths between 20 and 60 m are investigated due to technological restrictions in the installation and operation of the OWT and WEC [49,57,78]. Moreover, a quantitative analysis is done for six candidate sites in order to clarify the differences and advantages of the combined devices compared to the individual ones. The sites are selected from the authors' previous work [40,48], representing the most suitable locations considering both short-term fluctuation and long-term change in climate in the sustainability of resources, and named after the nearest city to them (Table 3).

Table 3. Characteristics and locations of the selected sites.

Sites name	Lat	Long	Water depth (m)	Distance to coast (Km)	WPD (W/m^2)	WPF (kW/m)
Hong Kong (HK)	21.85	114.5	55.2	47	627.24	7.85
Shanwei (SW)	22.25	115.65	57.7	46.5	819.74	7.82
Quanzhou (QZ)	24.6	119.25	58.2	41.7	1489.2	9.66
Fuzhou (FZ)	25.75	120.1	41.5	49.4	976.6	10.28
Wenzhou (WZ)	27.15	121.05	36	46.6	801.54	10.07
Zhoushan (ZS)	29.5	122.7	46.5	46.1	984.98	11.76

The annual energy production (AEP) is estimated for the single OWT, WEC, and their combination (Fig. 8). As Fig. 8 demonstrates, the wind has higher AEP than the wave due to the higher conversion efficiency of the OWT compared with the WEC. As WEC designs advance, higher conversion efficiency is expected. The results show that wind energy production increases from the western parts to the eastern parts of the domain and reaches the highest value (above 35 GWh/year) in the Taiwan Strait and then slightly decreases. However, the wave energy production increases toward the eastern parts and encounters the maximum on the Zhejiang coast. The combined energy production considerably increases in most areas in Fig. 8c, especially in the areas with high synergy, such as the Zhejiang coast. The AEP values in the six candidate sites are highlighted in Table 4 to clarify the improvements. As shown in Table 4, the energy production using the combined wind and wave resources is increased 22–36% and 374-549% compared to the single OWT and WEC, respectively. The high AEP (nearly 40 GWh/year) is in the sites FZ, QZ, and ZS, while the largest contribution of wave energy is in ZS.

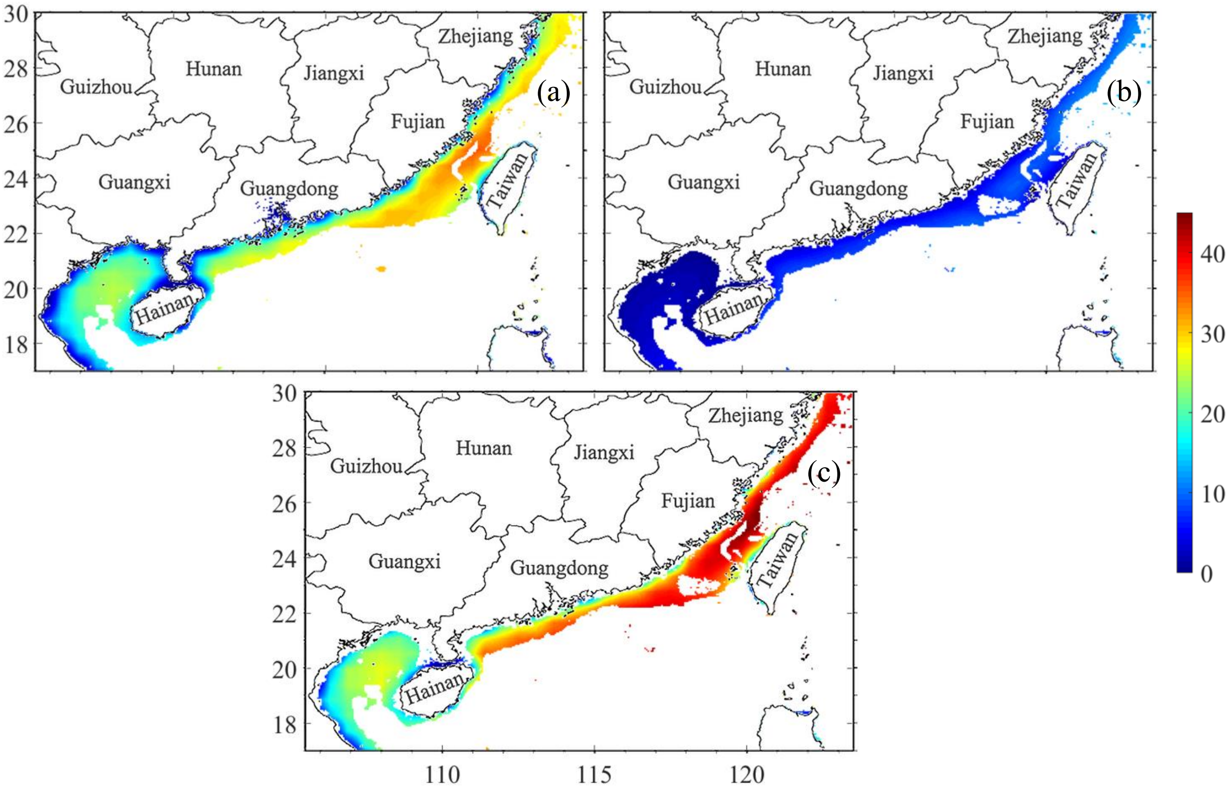

Fig. 8. AEP (GWh) for (a) the OWT, (b) WEC, and (c) their combination in the areas with depths between 20 and 60 m.

Table 4. AEP for the OWT, WEC, and their combination in the selected sites.

Sites name	OWT only (GWh)	WEC Only (GWh)	Combined (GWh)	Increase rate compared to OWT /WEC only	
HK	25.41	7.75	33.16	30.49%	427.92%
SW	28.17	7.20	35.36	25.55%	491.27%
QZ	33.52	7.46	40.98	22.25%	549.48%
FZ	31.02	9.38	40.40	30.22%	430.81%
WZ	26.87	9.52	36.40	35.44%	382.12%
ZS	28.75	10.47	39.22	36.41%	374.67%

In Fig. 9, the results of the monthly energy production for the single OWT, WEC, and their combination in the candidate sites are reported. The temporal variability of the energy production on the monthly scale for the single OWT (blue bins), WEC (orange bins), and their combination (grey bins) for all considered sites is indicated in Fig. 9. According to Fig. 9, the highest combined variability is found in QZ, with the monthly energy production fluctuating between 2 and 4.7 GWh, in agreement with the high correlation between the two resources that characterizes the site in Fig. 5. In addition, the monthly energy production in the site is mainly dominated by wind resources, and the combined variability is upper than that for the single OWT. The lowest fluctuation of combined monthly energy production is recorded in ZS, ranging from 2.4 to 3.7 GWh, in agreement with the moderate correlation between the two resources that characterizes the site in Fig. 5. Furthermore, there is the highest wave contribution to the total energy production in ZS compared to other sites. Overall, it shows that with moving towards the eastern parts, the variability of combined devices on the monthly scale is reduced.

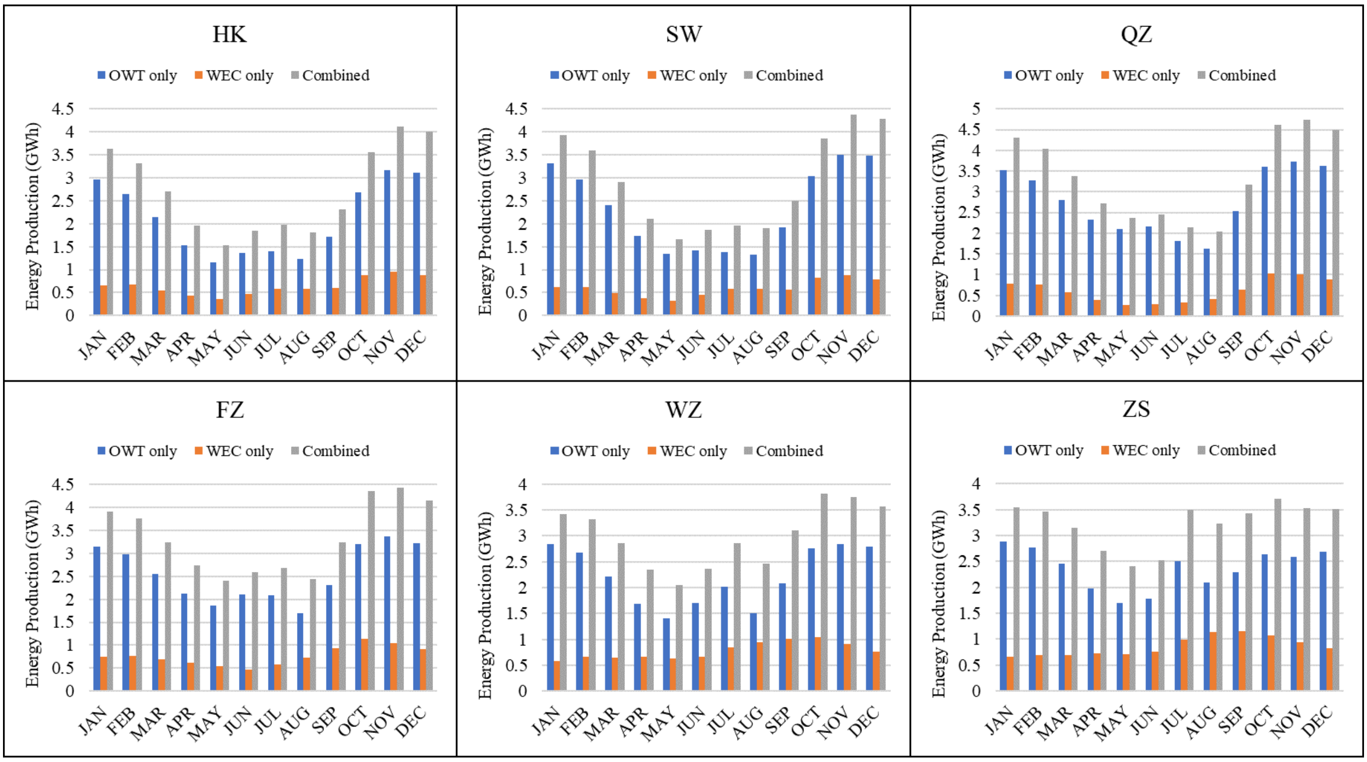

Fig. 9. Monthly energy production (GWh) for the OWT, WEC, and their combination in the candidate sites.

The annual mean values of *CF* for the single OWT, WEC, and their combination are displayed in

Fig. 10, and the quantitative analysis in the candidate sites is shown in Table 5. The patterns of *CF* are similar to that of AEP. According to Fig. 10, the *CF* for the OWT is about three times larger than that for the WEC. However, from a long-term perspective, the areas with high wave contribution are more attractive since OWTs technology has been mature and widely employed in the world, while it is not the case for WECs and hence, there is great potential for improvement in conversion efficiency in the future [23]. The *CF* for the combined devices is larger than that for the single WEC but lower than that for the OWT. However, the value is between 30% and 40%, which is still a satisfactory value on the coasts of Guangdong, Fujian and Zhejiang [23]. According to Table 5, QZ experiences the highest *CF* for both the OWT and combined device, while the difference between *CF* values is considerably high for the OWT and WEC.

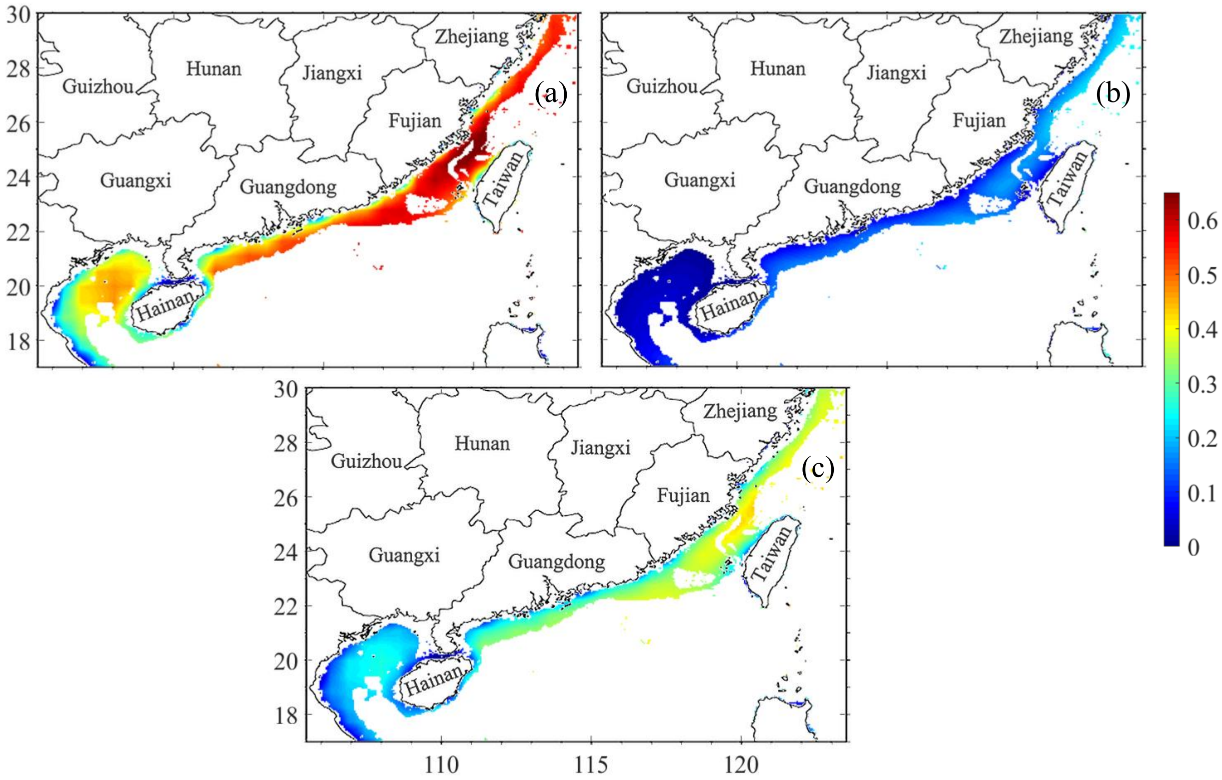

Fig. 10. Annual mean values of *CF* for (a) the OWT, (b) WEC, and (c) their combination in the areas with depths between 20 and 60 m.

Table 5. Annual mean values of *CF* (%) for the OWT, WEC, and combined OWT and WEC in the different candidate sites.

Sites name	OWT only	WEC only	Combined
HK	48.34	14.74	31.54
SW	53.59	13.69	33.64
QZ	63.78	14.19	38.98
FZ	59.03	17.84	38.43
WZ	51.13	18.12	34.63
ZS	54.70	19.92	37.31

One of the most considerable improvements from the joint exploitation of the available resource should be reducing intermittency, i.e., the possibility of periods of zero power output [51,69]. The zero production (the percentages of the hours with zero power output) for the OWT, WEC, and their combination are represented in Fig. 11. According to Fig. 11, the zero production of the OWT is low (less than 20%) in most areas except the Beibu Gulf and areas around Hainan, while the zero production of the WEC decreases with longitude along the south and southeast coasts of China. In addition, the zero production of the combined device can be reduced slightly compared to the individual devices on the Zhejiang coast. To clarify the reduction of intermittency for the combined device compared to the individual devices more clearly, the zero production (%) for the OWT, WEC, and their combination in candidate sites are highlighted in Table 6. In QZ, joint exploitation does not significantly reduce the zero production (it is nearly 1%). In contrast, in WZ and ZS, the zero production of the combined device is dropped nearly 7% compared to that of the OWT operating individually. It results from the high synergy of the two resources (Fig. 7d). Meanwhile, it is also noticeable that only 4% of zero production can be found in the site ZS using the combined approach.

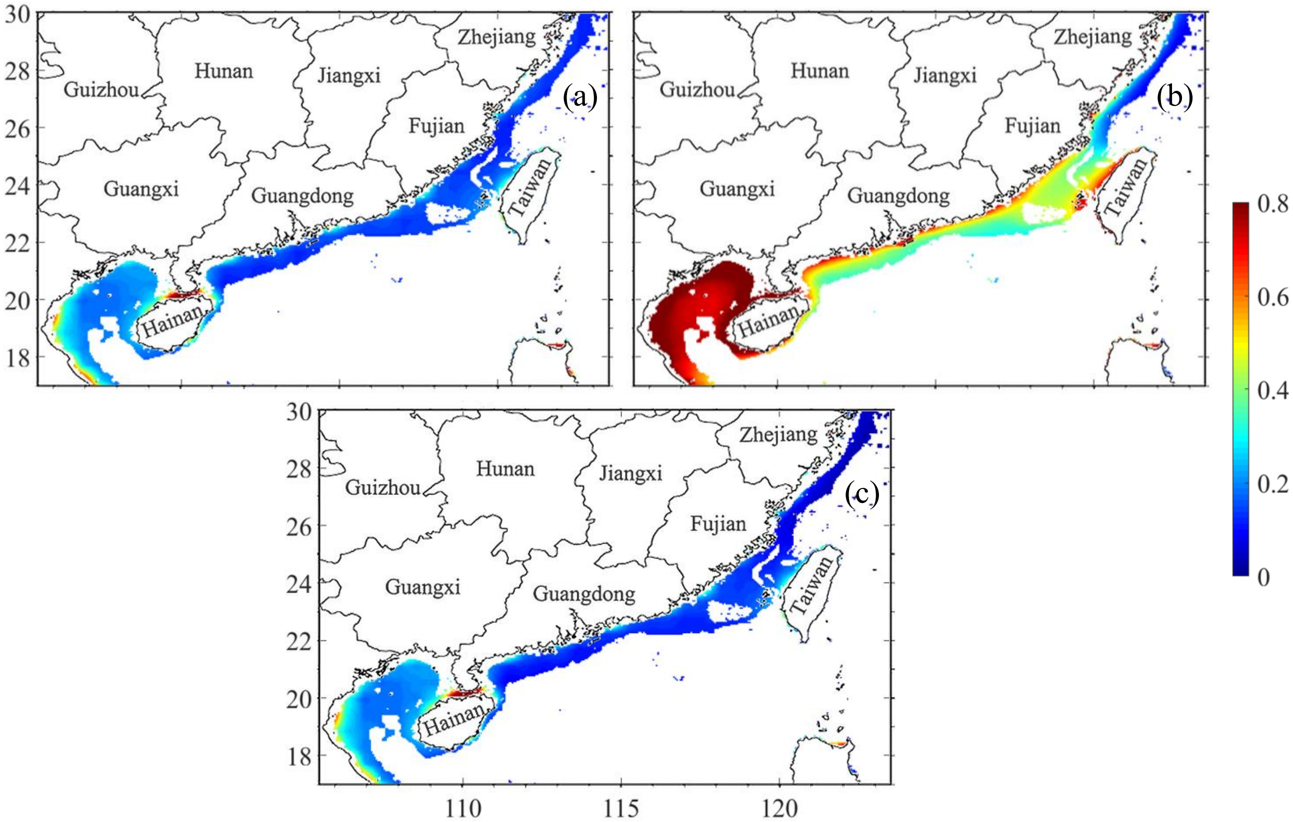

Fig. 11. Zero production for (a) the OWT, (b) WEC, and (c) their combination in the areas with depths between 20 and 60 m.

Table 6. Zero production (%) for the OWT, WEC, and their combination in the different candidate sites.

Sites name	OWT only	WEC only	Combined	Reduction compared to OWT /WEC only	
HK	14.035	34.613	11.664	2.371	22.949
SW	13.866	35.062	11.878	1.988	23.184
QZ	12.646	39.443	11.534	1.112	27.909
FZ	11.909	24.29	8.4259	3.4831	15.8641
WZ	14.946	18.022	7.4857	7.4603	10.5363
ZS	11.766	11.808	4.0486	7.7174	7.7594

Another crucial consideration for joint exploitation should be reducing the variability of resources in line with sustainability criteria. The variability of power output is quantified using *CoV* of power output, and shown in Fig. 12. The results indicate that the combined device generates less variable power than the OWT on the coasts of Guangdong and Zhejiang, and less variable power than the WEC in the Beibu Gulf, Taiwan Strait, and Fujian coast. Detailed analysis in the candidate sites is reported in Table 7. The variability related to the combined concepts decreases for all sites with respect to those evaluated considering the single OWT or WEC (with the exception of the site QZ, in which the variability of the combined device is slightly higher than that of the OWT).

The areas with high potential for planning the development of wind and wave resources should have high energy potential and low variability [3]. Hence, based on the results, Zhejiang coast should be introduced as a priority for joint wind-wave projects due to the high energy production (Fig. 8c), low variability (Fig. 12c) and low zero production (Fig. 11c).

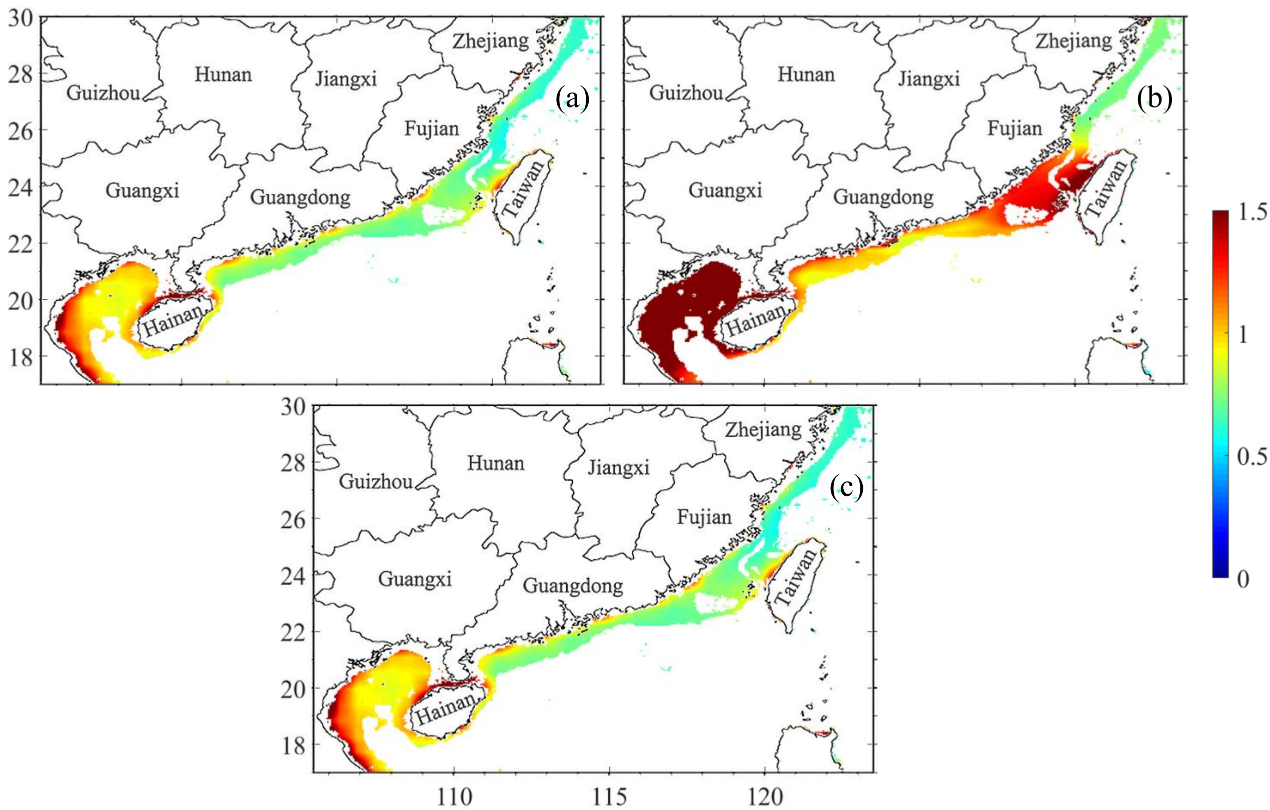

Fig. 12. *CoV* of power output for (a) the OWT, (b) WEC, and (c) their combination in the areas with depths between 20 and 60 m.

Table 7. *CoV* of power output for the OWT, WEC, and their combination at the different candidate sites.

Sites name	OWT only	WEC only	OWT and WEC	Reduction compared to OWT /WEC only	
HK	0.80135	0.88241	0.73721	0.06414	0.1452
SW	0.75255	0.95237	0.71009	0.04246	0.24228
QZ	0.63851	1.2011	0.65382	-0.01531	0.54728
FZ	0.67425	0.84202	0.6168	0.05745	0.22522
WZ	0.7858	0.72207	0.66069	0.12511	0.06138
ZS	0.72295	0.74772	0.61583	0.10712	0.13189

3.5 WWJE index considering both wind and wave correlation and synergy

Previously, wind and wave energy potential and their correlation have been applied to the investigation of the joint exploitation potential (e.g. [1,74]). However, the synergy has not been adequately considered in these studies. In addition, according to the analysis in the previous section and Refs. [24,25,69,70], the joint exploitation in the areas with low correlation and high synergy can reduce the variability and intermittency of power output. Hence, in order to include the synergy in the long-term to detect suitable areas for wind-wave joint exploitation, the new index called WWJE including energy potential, correlation, and synergy is defined in Eq. (10). The WWJE can be used for any other region and different resources combination after adjusting the weights and EGT.

The distributions of WWJE for both the whole domain and the nearshore areas are shown in Fig. 13, by setting $C_{wind}=C_{wave}=0.5$. The result shows that the southeast waters of Taiwan Island, which are characterized by high wind and wave power (Fig. 2), low correlation (Fig. 5), and high synergy (Fig. 7), experience the highest WWJE values. However, the continental shelf in the area is very narrow, which causes difficulty in developing wind-wave projects. Fig. 13b displays the WWJE in the nearshore areas of the domain, indicating the highest value on the Zhejiang coast. It is consistent with the results of qualitative analysis based on the specific combined device (Section 3.4). In addition, it is interesting to note that the areas, such as the southern part of the Taiwan Strait with very high wind (Fig. 2) and wave power potential (Fig. 6 in Ref. [48]), do not appear to be the best one for the combined exploitation due to the very high correlation and relatively moderate synergy between the two resources.

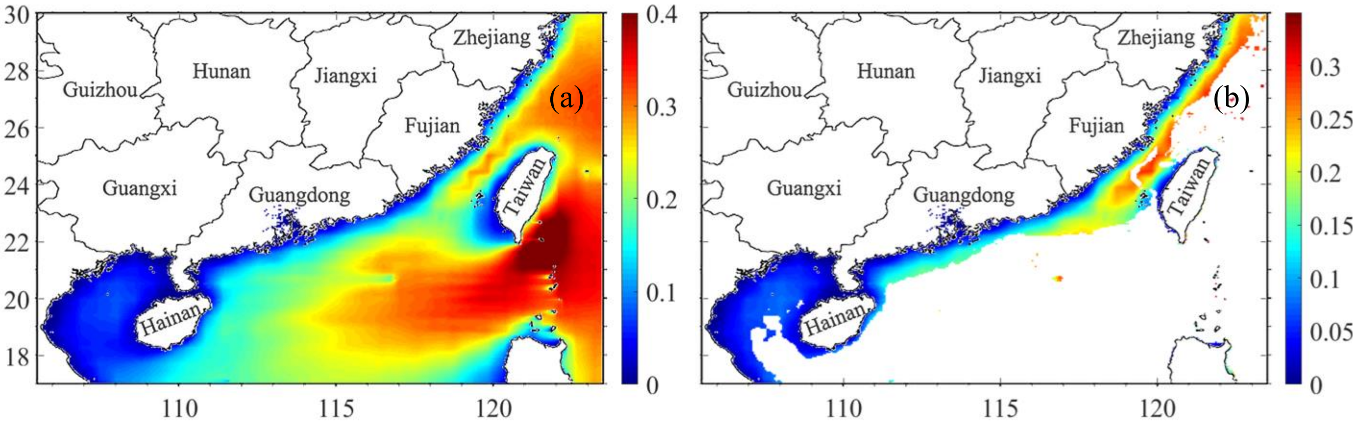

Fig. 13. The spatial distribution of WWJE index in (a) the entire domain and (b) the nearshore areas with depths below 60 m.

Finally, the influence of the different weighs of WPD and WPF is discussed. In the sensitivity tests, the selection of C_{wind} is from 0.1 to 0.9 with an interval of 0.2, and C_{wave} is from 0.9 to 0.1 with the same interval. The results of the sensitivity tests in the domain are shown in Fig. 14. According to the figure, there are similar spatial distributions by using different weights of WPD and WPF, while relatively large differences can be detected in the Taiwan Strait. It is because that there is a wide gap between wind and wave energy resources (Fig. 2) in the Taiwan Strait and hence it is sensitive to the choices of the weights. A large value of WWJE can be found in the Taiwan Strait when the weight of WPD is larger than that of WPF, while the value of WWJE is underestimated when the weight of WPF is larger than that of WPD.

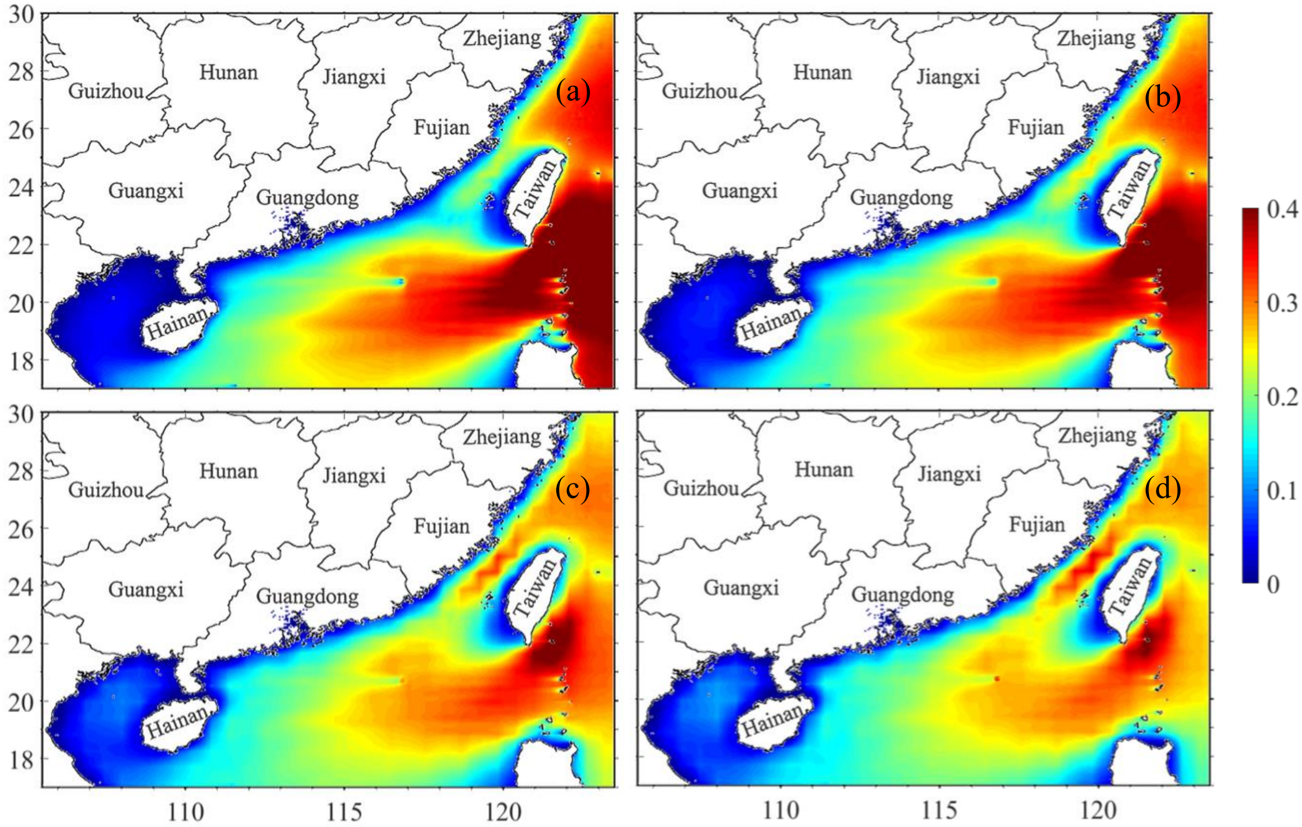

Fig. 14. The values of WWJE for different weight pairs for WPD and WPF : (a) (0.1, 0.9), (b) (0.3, 0.7), (c) (0.7, 0.3), (d) (0.9, 0.1) in the domain.

4. Summary and Conclusion

In this study, the 55-year offshore wind and wave datasets were employed to analyze the relation between two resources and to evaluate the joint exploitation potential along the south and southeast coasts of China. The correlation, complementarity and synergy of wind and wave energy were investigated. Moreover, the benefits of using combined devices were further analyzed in terms of enhanced energy production, reduced intermittency and variability. Finally, a new index was presented to help identify the most prospective sites for wind-wave combined exploitation based on the WPD, WPF, correlation, and synergy between the two resources.

The analysis indicated that the two resources are abundant in the domain, although with a slightly different spatial distribution. The Taiwan Strait is a golden area for offshore wind resources, while the hotspot area of wave resources is in the southeast waters of Taiwan Island. The correlation analysis indicated that the southern part of the Taiwan Strait has a very high correlation between wind and wave, whereas moderate correlation can be found in the southeast waters of the Taiwan and Zhejiang Coast. Moreover, the Zhejiang coast and east waters of Taiwan Island experience considerably high synergy between wind and wave.

The significant benefits of the wind-wave joint exploitation include higher energy production rate, lower variability of power output and less zero production. The results indicated that the AEP value increases by 22~35% with the use of the combined concepts, as compared to the single wind turbine in most areas, and the high AEP (nearly 40 GWh/year) appears in the offshore sites near FZ, QZ, and ZS. Besides, the reduction of variability and zero production can be found mainly on the Zhejiang coast characterized by relatively low correlation and high synergy.

Furthermore, based on the proposed WWJE index, the Zhejiang coast and northern part of the Taiwan Strait are the most attractive regions for wind-wave combined exploitation. On the other hand, the Beibu Gulf, with low energy potential and synergy and high correlation, is not recommended for further consideration for joint wind-wave projects. The WWJE index also suggests that the highest wind and wave energy potential should not be the determining factors. In contrast, the areas with moderate combined energy potential but lower correlation and higher synergy are more suitable for further assessment for development. The proposed index can be a useful tool for the decision-makers and investors of wind-wave projects, and the sensitivity analysis can provide different choices for investors considering relative importance of wind and wave development. Nevertheless, additional considerations such as economy, topography and environmental impacts should also be taken into account for future planning of wind-wave combined projects. The results of this study highlighted the importance of diversity in the renewable energy mix.

Acknowledgment

This research has been conducted under grant No. Skhl1807 supported by State Key Laboratory of Hydraulics and Mountain River Engineering, Sichuan University, and the grant from NSFC (52031002;51879237). Part of this work has been supported by the Hakubi Center for Advanced Research at Kyoto University, and JSPS Grants-in-Aid for Scientific Research (KAKENHI), grant No. 20K04705, supported by the Ministry of Education, Culture, Sports, Science, and Technology of Japan (MEXT). The authors are thankful to Japan Meteorological Agency (JMA) for providing JRA-55 dataset.

Reference

[1] Ferrari F, Besio G, Cassola F, Mazzino A. Optimized wind and wave energy resource assessment and offshore exploitability in the Mediterranean Sea. Energy 2020;190:116447. https://doi.org/10.1016/j.energy.2019.116447.

[2] Robertson B, Dunkle G, Gadasi J, Garcia-Medina G, Yang Z. Holistic marine energy resource assessments: A wave and offshore wind perspective of metocean conditions. Renewable Energy 2021;170:286–301. https://doi.org/10.1016/j.renene.2021.01.136.

[3] Kamranzad B, Lin P, Wen Y. Sustainability of wave energy resources in the South China Sea based on five decades of changing climate. Energy 2020;210:118604. https://doi.org/10.1016/j.energy.2020.118604.

[4] He J, Chan PW, Li Q, Lee CW. Spatiotemporal analysis of offshore wind field characteristics and energy potential in Hong Kong. Energy 2020;201:117622. https://doi.org/10.1016/j.energy.2020.117622.

[5] Esteban MD, Diez JJ, López JS, Negro V. Why offshore wind energy? Renewable Energy 2011;36:444–50. https://doi.org/10.1016/j.renene.2010.07.009.

[6] Sant'Anna de Sousa Gomes M, Faulstich de Paiva JM, Aparecida da Silva Moris V, Nunes AO. Proposal of a methodology to use offshore wind energy on the southeast coast of Brazil. Energy 2019;185:327–36. https://doi.org/10.1016/j.energy.2019.07.057.

[7] Clément A, McCullen P, Falcão A, Fiorentino A, Gardner F, Hammarlund K, et al. Wave energy in Europe: Current status and perspectives. Renewable and Sustainable Energy Reviews 2002;6:405–31. https://doi.org/10.1016/S1364-0321(02)00009-6.

[8] Liu Y, Li Y, He F, Wang H. Comparison study of tidal stream and wave energy technology development between China and some Western Countries. Renewable and Sustainable Energy Reviews 2017;76:701–16. https://doi.org/10.1016/j.rser.2017.03.049.

[9] Sasmal K, Waseda T, Webb A, Miyajima S, Nakano K. Assessment of wave energy resources and their associated uncertainties for two coastal areas in Japan. Journal of Marine Science and Technology (Japan) 2020. https://doi.org/10.1007/s00773-020-00781-y.

[10] Sarmiento J, Iturrioz A, Ayllón V, Guanche R, Losada IJ. Experimental modelling of a multi-use floating platform for wave and wind energy harvesting. Ocean Engineering 2019;173:761–73. https://doi.org/10.1016/j.oceaneng.2018.12.046.

[11] Astariz S, Iglesias G. The economics of wave energy: A review. Renewable and Sustainable Energy Reviews 2015;45:397–408. https://doi.org/10.1016/j.rser.2015.01.061.

[12] Astariz S, Vazquez A, Sánchez M, Carballo R, Iglesias G. Co-located wave-wind farms for improved O&M efficiency. Ocean and Coastal Management 2018;163:66–71. https://doi.org/10.1016/j.ocecoaman.2018.04.010.

[13] Pérez-Collazo C, Greaves D, Iglesias G. A review of combined wave and offshore wind energy. Renewable and Sustainable Energy Reviews 2015;42:141–53. https://doi.org/10.1016/j.rser.2014.09.032.

[14] Fusco F, Nolan G, Ringwood J V. Variability reduction through optimal combination of

wind/wave resources - An Irish case study. Energy 2010;35:314–25. https://doi.org/10.1016/j.energy.2009.09.023.

[15] Astariz S, Iglesias G. Output power smoothing and reduced downtime period by combined wind and wave energy farms. Energy 2016;97:69–81. https://doi.org/10.1016/j.energy.2015.12.108.

[16] Hu J, Zhou B, Vogel C, Liu P, Willden R, Sun K, et al. Optimal design and performance analysis of a hybrid system combing a floating wind platform and wave energy converters. Applied Energy 2020;269:114998. https://doi.org/10.1016/j.apenergy.2020.114998.

[17] Veigas M, Carballo R, Iglesias G. Wave and offshore wind energy on an island. Energy for Sustainable Development 2014;22:57–65. https://doi.org/10.1016/j.esd.2013.11.004.

[18] Erdinc O, Uzunoglu M. Optimum design of hybrid renewable energy systems: Overview of different approaches. Renewable and Sustainable Energy Reviews 2012;16:1412–25. https://doi.org/10.1016/j.rser.2011.11.011.

[19] Astariz S, Perez-Collazo C, Abanades J, Iglesias G. Hybrid wave and offshore wind farms: A comparative case study of co-located layouts. International Journal of Marine Energy 2016;15:2–16. https://doi.org/10.1016/j.ijome.2016.04.016.

[20] Astariz S, Iglesias G. The collocation feasibility index – A method for selecting sites for co-located wave and wind farms. Renewable Energy 2017;103:811–24. https://doi.org/10.1016/j.renene.2016.11.014.

[21] Rusu E, Onea F. A parallel evaluation of the wind and wave energy resources along the Latin American and European coastal environments. Renewable Energy 2019;143:1594–607. https://doi.org/10.1016/j.renene.2019.05.117.

[22] Stoutenburg ED, Jenkins N, Jacobson MZ. Power output variations of co-located offshore wind turbines and wave energy converters in California. Renewable Energy 2010;35:2781–91. https://doi.org/10.1016/j.renene.2010.04.033.

[23] Kalogeri C, Galanis G, Spyrou C, Diamantis D, Baladima F, Koukoula M, et al. Assessing the European offshore wind and wave energy resource for combined exploitation. Renewable Energy 2017;101:244–64. https://doi.org/10.1016/j.renene.2016.08.010.

[24] Gallagher S, Tiron R, Whelan E, Gleeson E, Dias F, McGrath R. The nearshore wind and wave energy potential of Ireland: A high resolution assessment of availability and accessibility. Renewable Energy 2016;88:494–516. https://doi.org/10.1016/j.renene.2015.11.010.

[25] Astariz S, Iglesias G. Selecting optimum locations for co-located wave and wind energy farms. Part II: A case study. Energy Conversion and Management 2016;122:599–608. https://doi.org/10.1016/j.enconman.2016.05.078.

[26] Azzellino A, Lanfredi C, Riefolo L, Contestabile P, Vicinanza D. Combined exploitation of offshore wind and wave energy in the Italian seas: A spatial planning approach. Frontiers in Energy Research 2019;7:1–15. https://doi.org/10.3389/fenrg.2019.00042.

[27] https://www.floatingpowerplant.com/products/

[28] http://www.pelagicpower.notechnology.html

[29] Liu HW, Ma S, Li W, Gu HG, Lin YG, Sun XJ. A review on the development of tidal current energy in China. Renewable and Sustainable Energy Reviews 2011;15:1141–6. https://doi.org/10.1016/j.rser.2010.11.042.

[30] Mirzaei A, Tangang F, Juneng L. Wave energy potential assessment in the central and

southern regions of the South China Sea. Renewable Energy 2015;80:454–70. https://doi.org/https://doi.org/10.1016/j.renene.2015.02.005.

[31] Zhou G, Huang J, Zhang G. Evaluation of the wave energy conditions along the coastal waters of Beibu Gulf, China. Energy 2015;85:449–57. https://doi.org/https://doi.org/10.1016/j.energy.2015.03.094.

[32] Zheng CW, Li CY. Variation of the wave energy and significant wave height in the China Sea and adjacent waters. Renewable and Sustainable Energy Reviews 2015;43:381–7. https://doi.org/https://doi.org/10.1016/j.rser.2014.11.001.

[33] Wang Z, Dong S, Li X, Soares CG. Assessments of wave energy in the Bohai Sea, China. Renewable Energy 2016;90:145–56. https://doi.org/https://doi.org/10.1016/j.renene.2015.12.060.

[34] Chen X, Wang K, Zhang Z, Zeng Y, Zhang Y, O'Driscoll K. An assessment of wind and wave climate as potential sources of renewable energy in the nearshore Shenzhen coastal zone of the South China Sea. Energy 2017;134:789–801. https://doi.org/https://doi.org/10.1016/j.energy.2017.06.043.

[35] Wang Z, Duan C, Dong S. Long-term wind and wave energy resource assessment in the South China sea based on 30-year hindcast data. Ocean Engineering 2018;163:58–75. https://doi.org/https://doi.org/10.1016/j.oceaneng.2018.05.070.

[36] Lin Y, Dong S, Wang Z, Guedes Soares C. Wave energy assessment in the China adjacent seas on the basis of a 20-year SWAN simulation with unstructured grids. Renewable Energy 2019;136:275–95. https://doi.org/https://doi.org/10.1016/j.renene.2019.01.011.

[37] Zheng C, Pan J, Li J. Assessing the China Sea wind energy and wave energy resources from 1988 to 2009. Ocean Engineering 2013;65:39–48. https://doi.org/https://doi.org/10.1016/j.oceaneng.2013.03.006.

[38] Wu Y, Tao Y, Zhang B, Wang S, Xu C, Zhou J. A decision framework of offshore wind power station site selection using a PROMETHEE method under intuitionistic fuzzy environment: A case in China. Ocean and Coastal Management 2020;184:105016. https://doi.org/10.1016/j.ocecoaman.2019.105016.

[39] Li D, Geyer B, Bisling P. A model-based climatology analysis of wind power resources at 100-m height over the Bohai Sea and the Yellow Sea. Applied Energy 2016;179:575–89. https://doi.org/10.1016/j.apenergy.2016.07.010.

[40] Wen Y, Kamranzad B, Lin P. Assessment of long-term offshore wind energy potential in the south and southeast coasts of China based on a 55-year dataset. Energy 2021;224:120225. https://doi.org/10.1016/j.energy.2021.120225.

[41] Shu ZR, Li QS, He YC, Chan PW. Observations of offshore wind characteristics by Doppler-LiDAR for wind energy applications. Applied Energy 2016;169:150–63. https://doi.org/10.1016/j.apenergy.2016.01.135.

[42] Hong L, Möller B. Offshore wind energy potential in China: Under technical, spatial and economic constraints. Energy 2011;36:4482–91. https://doi.org/10.1016/j.energy.2011.03.071.

[43] Dong S, Gong Y, Wang Z, Incecik A. Wind and wave energy resources assessment around the Yangtze River Delta. Ocean Engineering 2019;182:75–89. https://doi.org/https://doi.org/10.1016/j.oceaneng.2019.04.030.

[44] Wan Y, Fan C, Dai Y, Li L, Sun W, Zhou P, et al. Assessment of the Joint Development

Potential of Wave and Wind Energy in the South China Sea. Energies 2018;11. https://doi.org/10.3390/en11020398.
[45] Renewables Consulting Group. GWEC,2020. Global Offshore Wind Report 2020 2020:130.
[46] OES. Annual Report an Overview of Ocean Energy Activities in 2019. The Executive Committee of Ocean Energy Systems 2019:152.
[47] Ebita A, Kobayashi S, Ota Y, Moriya M, Kumabe R, Onogi K, et al. The Japanese 55-year reanalysis “JRA-55”: An Interim Report. Scientific Online Letters on the Atmosphere 2011;7:149–52. https://doi.org/10.2151/sola.2011-038.
[48] Kamranzad B, Lin P, Iglesias G. Combining methodologies on the impact of inter and intra-annual variation of wave energy on selection of suitable location and technology. Renewable Energy 2021;172:697–713. https://doi.org/10.1016/j.renene.2021.03.062.
[49] Emeksiz C, Demirci B. The determination of offshore wind energy potential of Turkey by using novelty hybrid site selection method. Sustainable Energy Technologies and Assessments 2019;36:100562. https://doi.org/10.1016/j.seta.2019.100562.
[50] Lavidas G. Selection index for Wave Energy Deployments (SIWED): A near-deterministic index for wave energy converters. Energy 2020;196:117131. https://doi.org/10.1016/j.energy.2020.117131.
[51] Gaughan E, Fitzgerald B. An assessment of the potential for Co-located offshore wind and wave farms in Ireland. Energy 2020;200:117526. https://doi.org/10.1016/j.energy.2020.117526.
[52] Kamranzad B, Takara K. A climate-dependent sustainability index for wave energy resources in Northeast Asia. Energy 2020;209:118466. https://doi.org/10.1016/j.energy.2020.118466.
[53] Tsujino H, Urakawa S, Nakano H, Small RJ, Kim WM, Yeager SG, et al. JRA-55 based surface dataset for driving ocean–sea-ice models (JRA55-do). Ocean Modelling 2018;130:79–139. https://doi.org/10.1016/j.ocemod.2018.07.002.
[54] Arshad M, Ma X, Yin J, Ullah W, Liu M, Ullah I. Performance evaluation of ERA-5, JRA-55, MERRA-2, and CFS-2 reanalysis datasets, over diverse climate regions of Pakistan. Weather and Climate Extremes 2021;33:100373. https://doi.org/10.1016/j.wace.2021.100373.
[55] Kobayashi S, Ota Y, Hrada Y, Ebita A, Moriya M, Onoda H, et al. The JRA-55 Reanalysis: General Specifications and Basic Characteristics. Journal of the Meteorological Society of Japan Ser II 2015;93:5–48. https://doi.org/10.2151/jmsj.2015-001.
[56] Booij N, Ris RC, Holthuijsen LH. A third-generation wave model for coastal regions: 1. Model description and validation. Journal of Geophysical Research: Oceans 1999;104:7649–66. https://doi.org/10.1029/98JC02622.
[57] Veigas M, López M, Romillo P, Carballo R, Castro A, Iglesias G. A proposed wave farm on the Galician coast. Energy Conversion and Management 2015;99:102–11. https://doi.org/10.1016/j.enconman.2015.04.033.
[58] https://www.thewindpower.net/store_actor_en.php?id_type=5.
[59] Soukissian TH, Karathanasi FE, Zaragkas DK. Exploiting offshore wind and solar resources in the Mediterranean using ERA5 reanalysis data. Energy Conversion and Management 2021;237:114092. https://doi.org/10.1016/j.enconman.2021.114092.
[60] Silva AR, Pimenta FM, Assireu AT, Spyrides MHC. Complementarity of Brazils hydro and

offshore wind power. Renewable and Sustainable Energy Reviews 2016;56:413–27. https://doi.org/10.1016/j.rser.2015.11.045.

[61] Ren G, Wan J, Liu J, Yu D. Characterization of wind resource in China from a new perspective. Energy 2019;167:994–1010. https://doi.org/10.1016/j.energy.2018.11.032.

[62] Hsu SA, Meindl EA, Gilhousen DB. Determining the Power-Law Wind-Profile Exponent under Near-Neutral Stability Conditions at Sea. Journal of Applied Meteorology 1994:757–65.

[63] Shu ZR, Li QS, Chan PW. Investigation of offshore wind energy potential in Hong Kong based on Weibull distribution function. Applied Energy 2015;156:362–73. https://doi.org/10.1016/j.apenergy.2015.07.027.

[64] Widén J. Correlations between large-scale solar and wind power in a future scenario for Sweden. IEEE Transactions on Sustainable Energy 2011;2:177–84. https://doi.org/10.1109/TSTE.2010.2101620.

[65] Richardson DB, Harvey LDD. Strategies for correlating solar PV array production with electricity demand. Renewable Energy 2015;76:432–40. https://doi.org/10.1016/j.renene.2014.11.053.

[66] Liu Y, Xiao L, Wang H, Dai S, Qi Z. Analysis on the hourly spatiotemporal complementarities between China's solar and wind energy resources spreading in a wide area. Science China Technological Sciences 2013;56:683–92. https://doi.org/10.1007/s11431-012-5105-1.

[67] Santos-Alamillos FJ, Pozo-Vázquez D, Ruiz-Arias JA, Lara-Fanego V, Tovar-Pescador J. Analysis of spatiotemporal balancing between wind and solar energy resources in the southern Iberian Peninsula. Journal of Applied Meteorology and Climatology 2012;51:2005–24. https://doi.org/10.1175/JAMC-D-11-0189.1.

[68] Li Y, Agelidis VG, Shrivastava Y. Wind-solar resource complementarity and its combined correlation with electricity load demand. 2009 4th IEEE Conference on Industrial Electronics and Applications, ICIEA 2009 2009:3623–8. https://doi.org/10.1109/ICIEA.2009.5138882.

[69] Prasad AA, Taylor RA, Kay M. Assessment of solar and wind resource synergy in Australia. Applied Energy 2017;190:354–67. https://doi.org/10.1016/j.apenergy.2016.12.135.

[70] Soukissian TH, Karathanasi FE, Zaragkas DK. Exploiting offshore wind and solar resources in the Mediterranean using ERA5 reanalysis data. Energy Conversion and Management 2021;237:114092. https://doi.org/10.1016/j.enconman.2021.114092.

[71] Weiss CVC, Guanche R, Ondiviela B, Castellanos OF, Juanes J. Marine renewable energy potential: A global perspective for offshore wind and wave exploitation. Energy Conversion and Management 2018;177:43–54. https://doi.org/10.1016/j.enconman.2018.09.059.

[72] Kamranzad B, Hadadpour S. A multi-criteria approach for selection of wave energy converter/location. Energy 2020;204:117924. https://doi.org/10.1016/j.energy.2020.117924.

[73] Wan Y, Zheng C, Li L, Dai Y, Esteban MD, López-Gutiérrez JS, et al. Wave energy assessment related to wave energy convertors in the coastal waters of China. Energy 2020;202. https://doi.org/10.1016/j.energy.2020.117741.

[74] Astariz S, Iglesias G. Selecting optimum locations for co-located wave and wind energy farms. Part I: The Co-Location Feasibility index. Energy Conversion and Management 2016;122:589–98. https://doi.org/10.1016/j.enconman.2016.05.079.

[75] Nie B, Li J. Technical potential assessment of offshore wind energy over shallow continent shelf along China coast. Renewable Energy 2018;128:391–9. https://doi.org/10.1016/j.renene.2018.05.081.

[76] Wan Y, Fan C, Dai Y, Li L, Sun W, Zhou P, et al. Assessment of the joint development potential of wave and wind energy in the South China sea. Energies 2018;11:1–26. https://doi.org/10.3390/en11020398.

[77] Lund H. Large-scale integration of optimal combinations of PV, wind and wave power into the electricity supply. Renewable Energy 2006;31:503–15. https://doi.org/10.1016/j.renene.2005.04.008.

[78] Chen CQ, Zheng L, Zhou JL, Zhao H. Persistence and risk of antibiotic residues and antibiotic resistance genes in major mariculture sites in Southeast China. Science of the Total Environment 2017;580:1175–84. https://doi.org/10.1016/j.scitotenv.2016.12.075.